The genetic architecture of local adaptation in a cline

Fabien Laroche[1*], Thomas Lenormand[2]

Affiliations:

[1] UMR 1201 Dynafor, Univ Toulouse, INRAE, INPT, EI PURPAN, Castanet-Tolosan, France

[2] CEFE, Univ Montpellier, CNRS, EPHE, IRD, Montpellier, France.

*Correspondence to: fabien.laroche@inrae.fr

Abstract

Local adaptation is pervasive. It occurs whenever selection favors different phenotypes in different environments, provided that there is genetic variation for the corresponding traits and that the effect of selection is greater than the effect of drift and migration. In many cases, ecologically relevant traits are quantitative and controlled by many genes. It has been repeatedly proposed that the within genome localization of these genes may not be random, but could be an evolved feature. In particular, the clustering of local adaptation genes may be theoretically expected and has been observed in several situations. Previous theory has focused on two-patches or island-continent models to investigate this phenomenon, reaching the conclusion that such clustering could evolve, but in relatively limited conditions. In particular, it required that migration rate was neither too low nor too large and that the full optimization of trait values could not be eventually achieved by a mutation at a single locus. Here, we investigate this question in spatially continuous space with distance-limited dispersal. We find that clustering of local-adaptation genes is pervasive within clines during both the establishment phase of local adaptation and the subsequent "reconfiguration" phase where different architectures compete with each other. We also show that different fitness functions relating trait to fitness have a strong impact on the overall dynamics and resulting architecture.

Introduction

Recombination is a key trait for sexual eukaryotes. Genome wide recombination rates are thought to evolve to limit selective interference and increase the efficacy of natural selection (Otto and Lenormand 2002; Otto 2009). Beyond this global pattern, it has been suggested that low recombination rate within genome could evolve locally to preserve particularly favorable genetic associations. This type of argument applies to sex differences in recombination (Lenormand 2003; Sardell and Kirkpatrick 2020), to inversions capturing loci with strong epistasis (Schwander et al. 2014; Charlesworth 2016), or to loci involved in local adaptation (Pylkov et al. 1998; Lenormand and Otto 2000; Kirkpatrick and Barton 2006). The latter in particular has received a lot of attention, as local adaptation is a ubiquitous phenomenon, and as "genomic islands" of divergence are sometimes, but not always, observed among differentiated populations (reviewed in Nosil et al. 2009; Strasburg et al. 2012). These "genomic islands" may however not result from the evolution of linkage. Instead, they can be relicts of a divergence built by independent evolutionary history of populations. In this case they appear simply because of the erosion of this divergence around selected loci (Barton and Hewitt 1989). Because of these different scenarios, the interpretation and evolutionary significance of such genomic islands are difficult to empirically establish. In addition to this empirical difficulty, the theory has not considered the case of spatially explicit models, where dispersal may be distance limited. Yet, in many situations, local adaptation may take place in a continuous space with a mosaic of different habitats. We investigate this case in this paper.

Local adaptation generally favors lower recombination because migration between habitats leads to positive genetic associations among loci involved in adaptation to these habitats. In this circumstance, lowering recombination rates preserves combinations of alleles that are locally beneficial, improves the response to selection, and reduces the migration load. Modifier models have been used to make this formal argument (Pylkov et al. 1998; Lenormand and Otto 2000; Lenormand 2012), however these general models do not investigate specific mechanisms by which local adaptation loci could evolve to be in tighter linkage. This could occur for several proximal reasons: (1) a local reduction in recombination rate, for instance through the occurrence of a chromosomal rearrangement (Kirkpatrick and Barton 2006; Yeaman 2013), (2) an aggregated recruitment of locally adapted alleles during adaptation to a new environment (Flaxman et al. 2013; Yeaman et al. 2016), (3) or competition between more or less aggregated genetic architectures conferring the same trait values (Yeaman and Whitlock 2011).

We focus here on mechanisms (2) and (3). We term mechanism 2 "emergence" and mechanism 3 "reconfiguration", and we refer to them collectively as "the evolution of aggregate genetic architecture". Aggregation emergence has been studied using either two-patch (Flaxman et al. 2013) or continent-island (Yeaman et al. 2016) models. These models suppose that many loci can contribute to local adaptation to a new environment and they evaluate whether the first mutations contributing to this local adaptation tend to cluster. They conclude that this mechanism is unlikely to strongly bias towards aggregated architecture. This is essentially due to two reasons (Yeaman et al. 2016): first, there is a narrow range of migration where there is a substantial difference between the establishment probability of a new mutation linked or unlinked to an existing polymorphism. Second, this difference in establishment probability is greatest for new mutations of small effects that could not establish alone (being swamped by migration), but could establish if tightly linked to a large effect mutation. However, if a distribution of effects of new mutations is considered, local adaptation occurs mostly through large effect mutations and this phenomenon plays therefore a minor role. The authors note that this conclusion should also hold in spatially explicit models, such as stepping stone, because the region where migration constrains local adaptation is, in addition, geographically limited.

Aggregation reconfiguration has also been studied in a two-patch model (Yeaman and Whitlock 2011), where a trait is under stabilizing selection around different optima in different environments. Many loci are assumed to contribute to this trait, but only a handful of mutations are sufficient to achieve local adaptation in the new environment. Hence, the same phenotypic change can be achieved by very different combinations of mutations at different loci. This allows different genetic architecture to compete, and eventually evolve on the long term. Simulation results show that indeed, aggregated architectures evolve in this model, but like for emergence, it occurs in a limited range of migration. There is a threshold migration rate below which locally favored alleles can increase in frequency and contribute to local adaptation (hereafter, swamping limit). In the two patch models, aggregated architecture evolves roughly between the smallest and largest swamping limits of plausible mutations. In other words, only for migration rates allowing for polymorphism to persist at local adaptation loci, while maintaining substantial gene flow. Like for emergence, aggregation also depends on the distribution of phenotypic effect of mutations. In particular, if mutation effects can "stack up" on a single locus, the system can evolve to just one single locus, i.e. a concentrated, rather than aggregated architecture (Yeaman and Whitlock 2011).

Here, we reconsider the evolution of aggregated architecture for three reasons. First, as noted above, it has been suggested that aggregation should be less favored in spatially explicit models with distance-limited migration (at least through the reconfiguration phase). However, this general conclusion is unclear. In particular, the opposite may be true if the condition for local adaptation are less restrictive in spatially explicit models compared to two patch-models. With distance-limited migration, clines form between habitats, irrespective of the relative intensity of migration and selection, provided the geographical scale of habitats is larger than the scale of migration (Nagylaki 1975; Slatkin 1978). Hence, aggregated genetic architecture might evolve within these clines, for a broad range of migration values.

Second, the distribution of mutational effects seems to play a significant role during the emergence or reconfiguration of aggregation, but several contradictory effects are at play. If mutations of large effects are frequent compared to those of small effects, aggregation is less likely to evolve since fewer loci will be involved in local adaptation and indirect selection will likely play a weaker role in their establishment. At one extreme, if a single mutation can occur that confer perfect adaptation, indirect selection for tight linkage will necessarily play a limited role. Hence, studying aggregation requires imposing some constraint on the maximum effect of mutations, which prevents full 'stacking' to occur. Such constraint may also be more representative of the type of genetic variants observed for quantitative traits. Similarly, it would be interesting to clarify the role of small and large effect mutations during the reconfiguration phase. In particular, the opportunity for mutations of large effects could have antagonistic effects on aggregation evolution. They may initially favor aggregation by attracting small effect mutations around them. However, changing a given genetic architecture around a phenotypic optimum involves crossing a fitness valley, which is expected to be deeper when it involves swapping alleles with larger phenotypic effects. Aggregation during the reconfiguration phase may therefore be slower with mutations of large effects. Third, the condition of polymorphism tightly depends on the shape of fitness trade-off between habitats. In formal one-locus population genetics model, a general case can be considered, where the selection coefficient of alleles in each habitat are free parameters (Nagylaki 1975). Models of polymorphism based on mutations of small effect can consider various fitness trade-off (Ravigne et al. 2009; Débarre and Gandon 2010). Models investigating the evolution of genetic architecture made however more specific assumptions. In continent-island models (Yeaman et al. 2016), no trade-off needs to be considered (only effects in the island), but this is a rather specific and drastic simplification. In multilocus models where the fitness effect of mutations is directly considered

(instead of their phenotypic effect), a linear trade-off is often assumed (Flaxman et al. 2013). The fitness effect of alleles simply switch sign across habitats, irrespective of their magnitude. In models using stabilizing selection on a trait, the underlying shape of fitness trade-off is implicit, and depends on the specific fitness function considered. This is for instance left as a flexible parameter in Yeaman and Whitlock 2011, but not investigated in details (parameter γ in their eq. 1). With some fitness functions, the ratio of selection coefficient of alleles across habitats depend on the magnitude of the phenotypic effect of the mutation and on the current mean trait value of the population (compare Gaussian and Laplace fitness function sketched on Figs. 1 and 2). Hence, different fitness functions may initially change the relative contribution to local adaptation of mutation of large or small phenotypic effects, as they will exhibit different fitness asymmetries across habitats. Furthermore, these contributions may also change dynamically during the process of adaptation, especially when those fitness asymmetries depend on the current mean trait values in the population. Hence, assuming different fitness function will likely influence the relative contribution to local adaptation of mutations of large or small phenotypic effects, and therefore, as explained above, influence the initial and long-term dynamics of aggregation.

To address these issues, we investigate how genetic architecture evolves in a spatially continuous model with a small "pocket of adaptation". This spatial settings stands as the simplest extension of the continent-island model of adaptation considered in previous studies (Yeaman et al. 2016) to a spatially explicit context. We consider a two habitats model, in a 1-dimensional circular stepping stone. We consider stabilizing selection on a trait, and we consider that only two kinds of mutations can occur, either of small or large phenotypic effects. These effects are fixed and therefore full stacking of effects is not possible. This allows us to clearly isolate the role of mutations with different effect sizes on the evolution of aggregated architectures. Last, we consider two types of fitness functions (Gaussian and Laplace) to investigate whether the fitness function and the shape of trade-off matters for the evolution of aggregated architectures.

Methods

Model

We model the process of adaptation to a "pocket" (i.e. a finite, contiguous area) of habitat. We use a model with discrete time and space. We consider a one-dimensional landscape made of n patches regularly positioned on a circle, each with a constant number of individuals N.

Without loss of generality, we assume that the distance between two consecutive patches is one distance unit. This landscape is made of two habitats : n-l contiguous patches correspond to habitat 1, and l patches to habitat 2. Individuals express a phenotype z, which is under stabilizing selection around a different optimum value z_{opt} in the two habitats. We denote $z_{opt}(i)$ the optimum in patch i. We assume that $z_{opt}(i) = 0$ if patch i is in habitat 1 and $z_{opt}(i) = 1$ if patch i is in habitat 2 (Fig. 3A). We suppose that an individual fitness in patch i, denoted $w_i(z)$, declines with the deviation of the trait z from $z_{opt}(i)$:

$$w_i(z) = e^{-(\Omega|z-z_{opt}(i)|)^\gamma} \quad (1)$$

where Ω measures the intensity of stabilizing selection (which we will assume constant across all patches), and where γ controls the shape of this fitness function (following Yeaman and Whitlock 2011). We will focus on two cases: $\gamma = 2$, which is the widely used Gauss function and $\gamma = 1$, which we will refer to as the Laplace function (Fig. 1). An important difference between these two cases is that a phenotypic change ε around z_{opt} has a negligible effect on fitness at first order in the Gaussian case (where $w(z)=1 + O(\varepsilon^2)$), but not in the Laplace case (where $w(z)=1 - \Omega|\varepsilon| + O(\varepsilon^2)$). These fitness functions also implicitly determine the shape of fitness trade-off across environments (Fig. 2). We will see below why it matters.

Each generation, migration occurs according to the kernel Π illustrated on Fig. 3B. Π is a $n \times n$ matrix, whose elements Π_{ij} give the proportion of individuals from patch j that reach patch i after migration. This kernel depends on two parameters: the proportion of migrants leaving a patch (m) and the maximal migration distance (d). Among migrants, the variance of this kernel is $\sigma^2 = d(d+1)/3$). The total variance of this kernel is therefore $m\sigma^2$, with a kurtosis in the range $[9/(10m), 9/(5m)]$ for increasing values of d.

Individuals are hermaphroditic and they randomly mate within their patch. They are diploid and carry two chromosomes with L uniformly spaced loci determining the trait z (Fig. 3C). We suppose that the number of cross-over at meiosis follows a Poisson distribution of parameter r, the map length. Cross-over are then uniformly distributed on the chromosome. Each locus is tri-allelic, with effect 0, a or A on z, with $0 < a < A$. Effects of alleles and loci are additive on z. Small effect mutations (of effect a) reversibly occur at rate μ_a (mutation events $0 \rightarrow a$, $a \rightarrow 0$ occur with probability μ_a). Large effect mutations (of effect A) reversibly occur at rate μ_A.

Mutation events $a \rightarrow A$, $A \rightarrow a$ do not occur, and we consider that large effect mutations occur less frequently than small effect mutations (typically $\mu_A = \mu_a /1000$; see Table 1).

We consider a population initially fixed for the wild type alleles 0, and we follow adaptation to a new pocket of habitat 2 which requires the occurrence and spread of these small or large effect alleles a or A. We consider the case where there are more loci available than required to reach the new optimum $z_{opt} = 1$ in habitat 2. For instance with $a = 0.01$, $A = 0.1$, the optimal phenotype can be reached by either 5 loci fixed for large effect alleles or 50 loci fixed for small effect alleles (or any intermediate combination). If $L = 100$, as we typically use, there are thus 2- and 20-times as many available than required loci if optimal phenotype is achieved by only large or small effect alleles, respectively. We can therefore study whether the genetic architecture tends to evolve to be "aggregated", i.e. whether contributing loci to the phenotypic change in habitat 2 tend to be closer from each other on the chromosome than expected by chance.

Analyses and simulations

We first analytically investigate the condition for polymorphism in this model. This step is important to identify swamping limits for alleles with small or large effects. For simulations, we use Wright-Fisher approach, drawing each new individual from the previous generation. First, we determine the patch of origin of the parents of the focal individual (according to the migration kernel). Each parent is then sampled with replacement from this patch weighted by its fitness. One (possibly) recombinant gamete is sampled from each parent to form the new individual and this is repeated to reach N individuals in each patch. The corresponding code is written in Java programming language and source code is available at 10.5281/zenodo.6602165.

Simulations are initialized with all individuals having phenotype $z = 0$. We focus on two timescales, one corresponding to the initial phase of adaptation (to follow the emergence of aggregation), the other considering adaptation in the long term (to follow the reconfiguration phase). The initial phase of adaptation is defined as the period between initialization and the first time when the average phenotype in the patch located at the middle of habitat 2 reaches 90% of its long term average stationary value. This initial phase lasted typically less than 50'000 generations in our simulations. The long term phase extends beyond this initial phase, generally up to 400'000 generations, which was sufficient to visually observe a stationary regime in average phenotype at the middle of habitat 2 over the last 75% of the simulation time.

The time step at which the state of the system was recorded differed between our simulations of long term (one record every 4000 generations) and initial phase of adaptation (one record every 500 generations). Table 1 gives the parameter values used in the simulations.

Measure of aggregation

Many possible metrics can be used to measure aggregation. We opt for a measure based on spectral analysis. We use the vector $v_i = (v_{i1}, v_{i2}, \ldots, v_{iL})$ giving the population frequency of (say) small alleles for the L loci along the chromosome, in a given patch i. If 50 loci are fixed for small alleles, and that all these contributing loci are next to each other, this vector would look like a "square signal" (i.e. to a signal characterized by a very low frequency), whereas if the 50 loci are randomly scattered along the chromosome, this vector will look like "white noise". Hence, aggregation can be measured by the bias of the spectral density towards low signal frequencies. To do so, we first compute the spectral density s_f at signal frequency f using a discrete Fourier transform of v_i. We then measure a weighed signal frequency:

$$F_0 = \sum_{f=1}^{L/2} s_f f \qquad (2)$$

which we scale between the maximal (F_{max}) and minimal (F_{min}) values possible to achieve for a vector carrying the same elements than v_i, but in a different order. Low F_0 indicate that the spectral density is biased toward low signal frequencies. F_{max} measures white noise and is computed as an average over random permutation of v_i. F_{min} measures the maximal aggregation that could be reached, and is computed on a vector where all values in v_i are sorted. Hence the scaled measure of aggregation :

$$F = \frac{F_{max} - F_0}{F_{max} - F_{min}} \qquad (3)$$

is close to 0 when there is no aggregation (the weighed signal frequency is close to the value obtained on random permutations), whereas it is close to one when aggregation is maximal

(close to a square signal). Whether this aggregation significantly differs from zero can also be assessed by obtaining its distribution under the null hypothesis (i.e. over the different permutations of v_i). This metric can be computed on the population frequency vector of only small alleles, only large alleles, or both combined.

Results

Condition for polymorphism

We first consider the deterministic condition for the existence of a cline for an allele introduced in a monomorphic population where individuals have trait value z. We consider a mutation at one locus creating a new phenotype z_{mut}. When rare, the mutant gamete frequency within the n patches $x(t)=(x_1(t), x_2(t), \ldots, x_n(t))$ follows the linear recursion:

$$x(t+1) = D\Pi x(t) \tag{4}$$

where D is a $n\times n$ diagonal matrix such that $D_{ii} = w_i(z_{mut})/w_i(z)$. Denoting $\lambda(z,z_{mut})$ the dominant eigenvalue of $D\Pi$, the mutant can invade the population if and only if $\lambda(z,z_{mut}) > 1$. Linearizing for small phenotypic effects of mutants (i.e. with $z_{mut} = z + \zeta\varepsilon$ with $\varepsilon \to 0^+$ and $\zeta = \pm 1$), then, for $0 < z < 1$, we have

$$\lambda(z, z_{mut}) = 1 + \zeta\partial_2\lambda(z,z)\epsilon + \partial_2^2\lambda(z,z)\frac{\epsilon^2}{2} + O(\epsilon^2) \tag{5}$$

In appendix A, we give a general expression of this dominant eigenvalue in terms of the parameters of the model. For simplicity, here, we only focus on the 'semi-infinite' limit, when habitat 2 is kept at a constant size, while the size of habitat 1 is considered infinitely large ($n\to+\infty$, Nagylaki 1975). Define s_1 (resp. s_2) the value of $w_i'(z)/w_i(z)$ in patches within habitat 1 (resp. 2), and t_1 the value of $w_i''(z)/w_i(z)$ in patches within habitat 1, we obtain:

$$\partial_2\lambda(z,z) \to s_1 \tag{6a}$$

$$\partial_2^2\lambda(z,z) \to \frac{(s_2-s_1)^2 l^2}{3m\sigma^2} + t_1 \tag{6b}$$

We derive the condition for the existence of a cline in this model, taking Nagylaki's 1975 results as a comparison. In Nagylaki's model, space is continuous and migration described by diffusion. The key result is that the condition for the existence of a cline is determined by two combined dimensionless parameters (see box 2, fig. II in Lenormand 2002). The first, noted k, measures the relative scales of the spatial heterogeneity (the size of the pocket) and of the 'characteristic length' (sensu Slatkin 1973) of the system, which weighs the strength of selection relative to gene flow. The second, noted α, measures the fitness asymmetry between habitats. It is defined as the ratio of minus the "outer" (in habitat 1, the allele is selected against) and "inner" (in habitat 2, the allele is selected for) selection coefficients of the allele. This parameter must be positive, as the model only concerns alleles with a trade-off among habitats. The existence of a cline is not relevant in other cases. Results for the Laplace and Gauss fitness functions are detailed below, and summarized in fig. 4.

Laplace trade-off - When $\gamma = 1$, (6a) simplifies to $\partial_2\lambda(z,z) = -\Omega$ irrespective of z value in]0,1[. We therefore expect z to converge towards $z^* = 0$. Because $\partial_2\lambda(0,0^+) = -\Omega$, $z^* = 0$ cannot be invaded by small mutations (Fig. 4). Equation (6b) becomes:

$$\partial_2^2\lambda(0,0) \to \Omega^2\left(\frac{4l^2}{3m\sigma^2} + 1\right) > 0 \tag{7}$$

Combining this result with equation (5) and assuming that $l^2/(m\sigma^2)$ is large yields that a small but non infinitesimal mutant could invade $z^* = 0$ when:

$$k > \sqrt{3}/2 \tag{8}$$

where $k = l\sqrt{2\Omega\epsilon}/(2\sigma\sqrt{m})$ expressed as in Nagylaki 1975. Here, the half size of the pocket is $l/2$, the additive fitness effect of the allele is $\Omega\epsilon$, and the standard deviation of the migration kernel is $\sigma\sqrt{m}$. With the case of a Laplace trade-off, α, the ratio of outer and inner selection coefficients is 1, for any allele. The fitness advantage gained in one habitat is lost in the other. The threshold value for the existence of a cline $\sqrt{3/2} = 0.87$ is close to Nagylaki's value corresponding to this case ($k = \pi/4 = 0.79$). The accuracy of this result depends on k being sufficiently large for the threshold $\sqrt{3}/2$ to be attained with reasonably small mutation ε. Hence, with a Laplace fitness function, large effect mutations invade more easily. They have a smaller swamping limit than small effect mutations, as they are exposed to stronger selection (larger k), but have the same ratio of outer/inner selection coefficients ($\alpha = 1$).

Gauss trade-off - When $\gamma = 2$, (6a) simplifies to $\partial_2\lambda(z,z) = -2\Omega^2 z$. We therefore expect z to converge towards $z^* = 0$. However, contrary to the previous case, $\partial_2\lambda(0,0^+) = 0$, which entails that z^* can be invaded by small mutations if $\partial_2^2\lambda(0,0^+) > 0$ (evolutionary branching point). From (6b), this condition simplifies to:

$$k > \sqrt{3/2}\,\sqrt{\alpha} \tag{9}$$

where, here, the combined parameters are $k = l\Omega\sqrt{\varepsilon}/(\sigma\sqrt{(2m)})$ and $\alpha = \varepsilon/2$. This result is also close to Nagylaki's 1975 result (Eq 38 and 40a), where the swamping limit is approximately $\sqrt{\alpha}$ for small α (compared to ~$1.22\sqrt{\alpha}$ in Eq. 9). An important difference with the Laplace case is that the intensity of selection scales with the asymmetry between habitats ($\alpha = \varepsilon/2$). Mutations of smaller phenotypic effects are exposed to weaker selection but they enjoy a more favorable outer/inner ratio of selection coefficients compared to mutations of larger phenotypic effects. At the limit, for mutations of very small phenotypic effect, this ratio tends towards zero, meaning that mutations of very small effect enjoy an advantage in habitat 2, while suffering from virtually zero fitness decrease in habitat 1. This is caused by the fact that the Gaussian fitness function is flat around the optimum. The consequence is that swamping limits do not depend on the phenotypic effects of mutations: either all mutations can invade, or none (depending on whether $l\Omega/(\sigma\sqrt{m})$ is greater or lower than $\sqrt{3/2}$, respectively).

Contribution to local adaptation of small vs. large effect mutations

In both the Laplace and Gauss case, polymorphism cannot arise when the size of habitat 2 (l) drops below a critical threshold. However, a qualitative difference exists between the two cases regarding mutations of small vs. large phenotypic effects: with the Laplace trade-off, polymorphism requires mutations of large (i.e. non-infinitesimal) effect, but not with Gauss trade-off. Again, the key explanation for this difference is that with Gauss trade-off, the asymmetry of selection between habitats drops to 0 as mutant effect size decreases (Fig. 4), while it stays constant in the Laplace case Hence, we expect that mutations of smaller effects should contribute much more to local adaptation in the Gauss vs. Laplace case. This difference should be reinforced by the fact that mutations of small effects (of effect a) occur more frequently than mutations of large effects (of effect A). However, this prediction is mitigated by the fact that the invasion criteria computed above do not account for stochastic loss of beneficial mutations that occur when mutations are present in few copies. This last effect should particularly penalize mutations of small effects that are initially predicted to invade in the Gauss case and reduce the difference between Gauss and Laplace cases. To quantify these antagonistic effects, we can compare the rate of establishment of small versus large mutations in the two cases. A branching process approximation predicts that a mutant allele of phenotypic effect ε has a probability of establishment that is approximately $2(\lambda(z^*,z^*+\varepsilon) - 1)$. Therefore, after a period of t generations, when neglecting interactions among alleles and the global shift of background phenotype (i.e. all the alleles are still rare), we expect the number of established small and large effect alleles to be proportional to $\mu_a(\lambda(z^*,z^*+a) - 1)t$ and $\mu_A(\lambda(z^*,z^*+A) - 1)t$, respectively. Among established alleles, the proportion P_A of large effect mutations should then be approximately

$$P_A = 1/\left[1 + \frac{\mu_a}{\mu_A}\frac{\lambda(0,a) - 1}{\lambda(0,A) - 1}\right] \quad (10)$$

and the part of the phenotype caused by these large alleles Q_A should be approximately

$$Q_A = 1/\left[1 + \frac{a}{A}\,\frac{\mu_a}{\mu_A}\,\frac{\lambda(0,a)-1}{\lambda(0,A)-1}\right] \tag{11}$$

The gross phenotypic contribution of mutations of large effect is then given by $\bar{z}Q_A$.

Gauss trade-off - In this case,

$$\lambda(0,\varepsilon) - 1 = \partial_2^2\lambda(0,0^+)\,\varepsilon^2/2 \tag{12}$$

Hence, when a polymorphism is possible, the contribution of large alleles to the current phenotype should be approximately

$$Q_A = 1/\left[1 + \left(\frac{a}{A}\right)^3\,\frac{\mu_a}{\mu_A}\right] \tag{13}$$

which is constant and equal to 0.5 with the parameter values used in our simulations (where small effect mutations have a 10-times smaller phenotypic effect, but a thousand time higher mutation rate).

Laplace trade-off - In this case,

$$\lambda(0,\varepsilon) - 1 = -\Omega\varepsilon + \partial_2^2\lambda(0,0^+)\,\varepsilon^2/2 \tag{14}$$

Hence, the contribution of large alleles to the current phenotype should be approximately

$$Q_A = 1/\left[1 + \left(\frac{a}{A}\right)^2\,\frac{\mu_a}{\mu_A}\,\frac{2\Omega - \partial_2^2\lambda(0,0^+)\,a}{2\Omega - \partial_2^2\lambda(0,0^+)\,A}\right] \tag{15}$$

with $\partial_2^2\lambda(0,0^+)$ given by Eq. 7. When the size of habitat 2 is between the swamping limits of large and small effect mutations, the phenotype should initially be exclusively made of large

effect mutations. For sizes of habitat 2 larger than the swamping limit of small effects mutations, the contribution of large effect mutations should decrease when the size of habitat 2 increases (in Eq 15, Q_A decreases as $\partial_2{}^2\lambda(0,0^+)$ increases, for instance with increasing l).

Effect of "background trait value" - These relative contributions of mutations of small and large effects are computed initially, when the average phenotype in habitat 2 just begins to evolve towards its optimal value. However, during this process, a cline builds up, and the average trait value increases in habitat 2, but also in habitat 1, at least close to the boundary between habitats. In the Laplace case, this is not strongly consequential, as the fitness function is linear and its local slope does not depend on average trait values, at least until adding one mutation causes a phenotypic overshoot in habitat 2. However, this is more consequential in the Gauss case: the slope of the Gauss fitness function gets steeper as trait value increases (instead of being flat initially, see fig. 1). When the average trait value increases in the Gauss case, mutations of small effect no longer enjoy the benefit of having more favorable outer/inner ratio of selection coefficients. As we detail in appendix B, this favors the establishment of mutations of larger effects compared to the initial expectation, during the adaptation process . In particular, when the average trait value becomes larger than a threshold value, small alleles cannot invade anymore and only large alleles can pursue the adaptation process (until the phenotype becomes close to the optimum so that overshooting becomes a problem). Overall, this effect of "background trait value" leads to an underestimation, in eq. 13, of the contribution of large effect mutations in the Gauss case. This bias becomes lower when the size of habitat 2 increases, as counterselection outside habitat 2 becomes less and less important in this case.

Effect of "aggregation" - Last, the establishment rates computed above do not account for indirect selection and linkage disequilibria among several alleles. In the Laplace case, for a given pocket size, only mutations exceeding a given effect size can form a cline and contribute to local adaptation. However, we also expect that during the establishment of local adaptation, some small effect mutations that occur in close linkage (to one another or to large effect mutations) could also invade. At small timescales, this effect will mostly concern small effect mutations, that co-occur much more frequently than large effect mutations (assuming, as we do, that $\mu_a \gg \mu_A$). For instance, for a pair of mutations, cases of co-occurrence will scale with the square of mutation rate, which can be limiting at short time scales (Yeaman 2013). This aggregation bias should be particularly strong below the swamping limit of small effect mutations, where mutations of small effect can establish only if they are aggregated. This effect will also favor small effect mutations in the Gauss case by increasing the establishment

probability of co-occuring small-effect mutations that happen to be in close linkage. Overall, this effect of "aggregation" favors small effect mutations in both the Laplace and Gauss cases. It should lead to cluster of small effect mutations, possibly grouped around a large-effect mutations. Here too, this bias should decrease with increasing size of habitat 2, as indirect selection only matters within clines at the boundary between habitats, i.e. in a fraction of the landscape that becomes relatively less important when the size of habitat 2 increases.

Simulations of the initial phase of adaptation

Laplace trade-off - Our analytical computation of the invasion threshold for large alleles derived from equation (7) proved remarkably accurate (Fig. 5A). Below this critical threshold, there was no adaptation in our simulations. As predicted, large effect mutations dominate when the size of habitat 2 is below the swamping limit of small-effect mutations, but their contribution declines above this limit. Nevertheless, we observe that small-effect mutations contribute significantly to the establishment of local adaptation even below this limit. As expected, they show a clear signal of aggregation in this case, and this signal is stronger when computed on small and large effect mutations combined (Fig 5B). In fact, small-effect mutations form clusters grouped around large effect mutations that establish first. Fig 6A shows a typical example of this dynamics. This aggregation bias is maximal close to the swamping limit of large-effect mutations and declines with increasing size of habitat 2, as predicted. Because of this aggregation bias, the gross contribution of large effect mutations to the phenotype given by eq. 15 is largely overestimated.

Gauss trade-off – In the simulations shown on Fig. 5, the swamping limit of both small and large effect mutations is $l = 5.2$. However, we do not observe a clear swamping effect. Contrary to the Laplace case, the average trait value start to increase smoothly below this threshold (fig 5C). With the gauss fitness function, mutations initially enjoy an advantage in habitat 2, while suffering very limited fitness reduction in habitat 1. Hence, many alleles can persist long enough to generate a weak pattern of local adaptation. Large effect alleles at l=5 showed also a weak but significant aggregation (Fig. 5D), which may also contribute to this phenomenon. The contribution of large effect mutations from eq. 13 agrees well with the simulation results. The "background trait value" bias (which favor large effect mutations) tend to cancel the "aggregation" bias (which favor small effect mutations). The aggregation bias is particularly significant for intermediate sizes of habitat 2 above the swamping limit (fig. 5D). Fig 6B shows a typical example of this dynamics.

Simulation of long term adaptation

Laplace trade-off – We confirmed that our prediction of swamping limit is accurate (Fig. 7A). We do not observe a marked change in the contribution of small vs large effects to the adaptive phenotype compared to the initial phase. There is still an excess of large effect alleles compared to the control (where habitat 1 is absent), especially for sizes of habitat 2 close to the swamping limits. These large effect mutations do not show a significant pattern of aggregation at the end of this long-term adaptation phase (Fig. 7B). In contrast, the aggregation of small effect mutations, which was already present in the initial phase, reinforces in the long term and reaches extreme values. This strong aggregation patterns occur for all sizes of habitat 2, even if it tends, like in the initial phase, to be stronger for sizes of habitat 2 close to the swamping limits.

Gauss trade-off – We still observed weak local adaptation for sizes of habitat 2 below the swamping limit, with similar magnitude than during the initial phase of adaptation (Fig. 7C). For all the habitat 2 sizes above swamping limit, the proportion of adaptive phenotype due to large alleles markedly increased compared to the initial phase of adaptation (and became much higher than in control where habitat 1 is absent). On the long run, small effects mutations are replaced by large effect mutations. For intermediate sizes of habitat above the swamping limit, these large effect mutations become aggregated (fig. 7D). For larger habitat 2 sizes, this aggregation of large effect mutations disappears, and is replaced by a pattern of aggregation of the residual small effect alleles. These residual small effect mutations strongly cluster around large effect mutations (the combined measure of aggregation on small and large effect mutations is much larger than each taken separately, fig. 7D).

Discussion

Local adaptation and aggregation in spatially explicit model

Spatially explicit model with limited dispersal allow to maintain polymorphism for a broad range of parameter values. Provided the environment is "coarse-grained" compared to the scale of gene flow (i.e. the sizes of the different habitats is sufficiently large), habitats' cores are more preserved from gene flow compared to peripheral zones and clines form at the boundary between habitats. This phenomenon is not present in spatially implicit (two-patches or mainland-island) models of adaptation. Here, for a given migration rate, local adaptation to a given habitat is always possible if the spatial extension of this habitat is large enough. Of course, a direct one-to-one comparison is not possible between spatially implicit and spatially explicit models, since the spatially explicit model introduces the effect of distance and extra-parameters. However, the spatially explicit model does not lead to the qualitative appreciation that the conditions of polymorphism, and aggregation, are restricted to a small range of migration rate. As long as clines form at the boundary between habitats, recombination is selected against among alleles forming these clines in the few patches around the habitat boundary with alleles at intermediate frequency. Away from these clines, recombination is neutral since no polymorphism is present. Hence, these clines provide a stable context favoring recombination suppression (or equivalently aggregated architecture) on the long-term. We indeed observe the emergence of aggregated genetic architecture on the long term in these conditions. We observed this both through the initial recruitment of linked alleles (during the "emergence" of local adaptation), and through the long-term competition between differentially aggregated genetic architectures (in the "reconfiguration" phase).

Condition for the existence of clines

The condition of polymorphism in a spatially explicit model have been precisely worked out for a single locus using a diffusion approximation (Nagylaki 1975). In this population genetic model, the fitness effect of alleles in the different habitats are constant parameters. The local adaptation allele has a fixed positive selection coefficient in one habitat and a fixed negative selection coefficient in the other. The effect of the fitness trade-off (the ratio of selection coefficients outside versus inside the focal habitat) can be distinguished from the effect of the intensity of selection (the selection coefficient within the focal habitat): the effect of each parameter can be kept constant while the other one is varying. In this context, and for a given

fixed trade-off, the condition for the existence of cline differ between weakly and strongly selected alleles. Allele of large effect can more easily escape swamping and form clines.

In a quantitative genetic type of model, selection is parameterized differently. We use stabilizing selection on a trait with different optima in the different habitats. Selection is therefore determined by the difference in optimal phenotype across habitats, the intensity of stabilizing selection around each of these optima and the precise shape of the fitness function around them. The treatment of such models remains similar to population genetic models regarding the existence of a first cline at a single locus, without the complication of linkage and indirect selection (Fig 4). However, the use of a fitness function relating the trait value to the fitness allows combining the effect of several loci in a parsimonious way. With stabilizing selection, the fitness effect of an allele with a given phenotypic effect depends on other alleles, contrary to simple population genetic models. For instance, if the population is at the optimum trait value, a mutation increasing the trait value is deleterious. It would be beneficial if the population had a trait value well below the optimal value. In addition to this background effect, the precise shape of the fitness function also matters. There are indeed many possible functions that can be used to describe stabilizing selection. It is necessary to scale them in some ways to compare results with different functions. A natural way to scale them is to assume that the overall fitness difference between habitats is kept constant (i.e., such that irrespectively of the function used, the fitness drop of having, in one habitat, the phenotypic value optimal in another is the same). This scaling necessarily entails that alleles with a given phenotypic effect on the trait do not necessarily have the same fitness effect with the different functions, for a given average trait value in the population. This complicates the direct comparison for the conditions of polymorphism for given alleles in the different cases. However, beyond this scaling issue, we observe that the choice of this fitness function has a large qualitative impact on the condition of polymorphism. This qualitative difference arises because the fitness function makes a particular assumption on the way that the trade-off (the ratio of selection coefficients across habitats) varies with the intensity of selection (Fig. 2). In the Laplace fitness function, the trade-off is constant for alleles of small and large phenotypic effects, as long as the phenotypic effect does not overshoot the optimum, and the results are therefore very similar to the population genetic model where selection coefficients of alleles are constant parameters. There are conditions (of migration intensity and habitat size) where large effect alleles can form clines while small effect alleles cannot (Fig. 4). In the Gaussian fitness function, however, the fitness trade-off varies with the phenotypic effect of alleles and the intensity of selection. Intuitively,

we see that when the population mean phenotype is close to the value optimal outside the pocket, an allele of small effect has an advantage in the pocket, but very little deleterious effect outside (since the fitness function is flat near the optimum outside the pocket). It can therefore invade very easily. For an allele with a larger effect, the trade-off is less favorable (it starts having a deleterious effect outside the pocket), but it enjoys a stronger intensity of selection. These two effects cancel each other, with the consequence that it is an all-or-nothing phenomenon: either all alleles can form clines or none. This Gaussian case is equivalent to a population genetic model where the trade-off would vary with the intensity of selection (Fig 4).

Overall, the choice of the fitness function has a qualitative effect on the dynamic of local adaptation, especially regarding the relative contribution of alleles of small and large effects and their temporal dynamics (see section "Patterns of aggregation with different fitness functions below"). Previous models have considered various fitness function but have not explicitly shown that the choice of the fitness function had a qualitative effect on patterns of polygenic local adaptation when alleles of different phenotypic effects are considered.

Condition to switch towards more aggregated architecture

Once local adaptation is established, aggregation can arise by the replacement of a given architecture by another (a change in the effect size distribution of alleles and/or in their positions along the chromosome). This progress towards aggregation takes time because the transition between architectures involve crossing a fitness valley. Indeed, when the phenotype is near its optimal value in the focal habitat, introducing a new local adaptation allele is likely to be deleterious, as it will cause an overshoot in the mean trait value. Hence, the first step for switching from one configuration to another involves recruiting an allele that has a deleterious allele in the context in which it arises. Of course, this deleterious effect can be immediately compensated by a frequency change at another locus (to keep the phenotype close to its optimum value), but this is necessarily a two-step phenomenon, where the first step is not favorable. Here too, the difference between the fitness functions also has an important consequence on the long-term outcome. Contrary to the Laplace case, the Gauss fitness function is flat near the optimum, so that small deviations necessarily have small deleterious fitness effects in the focal habitat. Hence the fitness valley is shallower in the Gaussian case. A polymorphism of architecture is more easily maintained around an optimum with a flat fitness function. As a consequence, transition between architecture is more fluid and occurs at a much faster rate in the Gauss versus Laplace case. In the latter, transitions involving large

effect mutations are extremely difficult, and these alleles tend to be stable over very long period of time, even though small effect mutations can switch positions and end up forming large cluster around them. Again, this comparison is made scaling the overall fitness difference among habitats (as common in quantitative genetics models), and not the fitness effect of individual alleles (as common in population genetics models). When selection acts on a trait, the fitness effect of alleles depends on the context (the background trait value), and are therefore not directly scalable.

Patterns of aggregation with different fitness functions

The vast majority of models of selection involving an environmental shift use Gaussian fitness functions. This is the case for instance when studying a temporal environmental variation (e.g. Bürger and Lynch 1995; Gomulkiewicz and Houle 2009; Chevin et al. 2010; Matuszewski et al. 2015; Marshall et al. 2016; Anciaux et al. 2018). Spatial models of species range also most often use a Gaussian fitness function (e.g. Kirkpatrick and Barton 1997; Alleaume-Benharira et al. 2006; Bridle et al. 2010; Polechová and Barton 2015; Fouqueau and Roze 2021). Such fitness function have received various justification and validation (Lande 1976; Martin and Lenormand 2006a; Martin et al. 2007). This fitness function is most often used for convenience for maintaining a normal distribution of phenotypes within a population, or to model smooth stabilizing selection around an optimum. As explained above, the choice of a fitness function also implicitly determines the fitness effects of mutations across environments and the shape of fitness trade-off across environments (Martin and Lenormand 2006b, 2015). While comparative analysis tend to globally support Gaussian trade-off patterns around optima (Martin and Lenormand 2006b), it is difficult to empirically affirm that such trade-off are valid for all loci and alleles, especially for the small effect mutations that are difficult to study. the precise shape of fitness function has been shown to also be important in other circumstances. For instance the shape of fitness function away from optima is crucial for predicting demographic consequences of large departures from optimal phenotype in situation of rapid environmental change (Osmond and Klausmeier 2017). In any case, our results show that the dynamics and pattern of aggregation strongly depend on the fitness function used.

Although both fitness trade-offs readily lead to aggregation patterns, the underlying configurations of alleles of small and large effects, their dynamics, and the resulting genetic map qualitatively differed. These qualitative differences between the Gauss and Laplace fitness function are caused by the conditions of polymorphism that differ for alleles of small and large effect, as explained above. This effect is particularly strong initially, when alleles are recruited

to establish local adaptation. Here the crucial point is whether the fitness function is flat or not outside the pocket, which determines whether small effect alleles have initially a more favorable trade-off than large effect alleles. The other important dynamical difference occurs in the longer term and depends on the ease to switch among architectures. Here, the crucial point is whether the fitness function is flat or not inside the pocket, such that alternative architectures can evolve without having to cross a deep fitness valley.

Overall, with a Laplace trade-off, aggregation stems from the fact that small alleles tend to aggregate along few, non-aggregated large alleles, hence creating several small, but stable, chromosomal islands of adaptation around each of those large allele. This effect is exacerbated when the pocket size is above the swamping limit of large effect alleles but below the swamping limit of small effect alleles. In this case, clines of small effects alleles emerge right from the beginning, as long as these alleles occur near large effect ones, and enjoy strong indirect selection. During this emergence phase, the interplay between the probability of invasion of small and large alleles and the hitch-hiking effects lead to a (relatively minor) non-linear change in the relative proportion of small vs. large effect alleles as the size of the habitat increases (Fig 5A, Appendix B). Because reconfiguration is slow with a Laplace fitness function, this effect is still present in the long term (Fig 7A). Overall, reconfiguration of the genetic architecture is markedly slower than in the Gaussian case, and particularly rare regarding alleles with large effect sizes. As a result, the genetic architecture remains remarkably stable in time under this regime.

With a Gauss trade-off, all the alleles tend to aggregate together irrespective of their effect size, while concentration (i.e. replacement of several small alleles by a large one) reinforces in time. This often leads to a single chromosomal island of adaptation in the long-term. Because of this concentration, effect sizes of adaptive alleles within the pocket were markedly higher with a Gaussian than with a Laplace fitness trade-off in the long term (Fig 7A-C). Like for the Laplace case, there is initially a (relatively minor) non-linear change in the relative proportion of small vs. large effect alleles as the size of the habitat increases (Fig 5C, Appendix B). However, this effect disappears in the long term since reconfiguration occurs quite rapidly (Fig 7C).

Empirically, if the resolution of the genetic map is low, small chromosomic islands mentioned above may appear as single loci and aggregation may be overlooked. Therefore, chromosomal islands of adaptation may be more conspicuous under the Gauss trade-off, unless the concentration process allows for stacking all the necessary phenotypic effect on a single allele (Yeaman and Whitlock 2011). In contrast, under the Laplace trade-off, the local adaptation

alleles may appear as scattered QTLs with large effect sizes. With a high resolution, however, alleles of small effect may be found surrounding these large effects loci. These expectations of course neglect that the architecture could also evolve because of chromosomal rearrangements (e.g. inversions) or local modifications of recombination rates (Lenormand and Otto 2000; Kirkpatrick and Barton 2006; Bürger and Akerman 2011; Lenormand 2012; Yeaman 2013; Charlesworth and Barton 2018). The importance of these secondary modifications of recombination ultimately depend on their relative rate of occurrence compared to the rate of architecture reconfiguration that we describe. In particular, they may play a stronger role in the Laplace case, where large effect alleles are stable on the long term and fail to consistently aggregate. However, these relative dynamics would require to be specifically investigated.

Comparison to previous studies

In addition to the differences associated with considering a spatially explicit model with distance limited dispersal, there are several points to discuss in comparison to previous studies on local adaptation and genetic aggregation. First, all studies do not consider both the emergence and the reconfiguration phases in the process of aggregation. The two combine, and the long term outcome depends on both. Second, all studies do not consider a fitness function relating trait to fitness, considering e.g. a set of loci with mutations with a constant effect. Stabilizing selection on a trait introduces the complication that the effect of alleles depends on the background and vary as local adaptation emerges. This can lead to very different outcomes. Third, models of local adaptation do not necessarily compare different shapes of fitness trade-off, or do so using cases that are apparently different, yet similar where it matters most. For instance Débarre and Gandon (2010) explored a wide range of trade-off functions in a two patch model. However, these functions are all similar on a critical aspect : their derivative of log-fitness close to optima is always 0. In that sense, all the trade-offs considered in that study are comparable to the Gaussian trade-off here, which explains why they did not find a strong effect of the shape of the fitness trade-off on the pattern of local adaptation. Last, and this is a related point, the different studies have not systematically explored the effect of different fitness functions, even when they considered a flexible model allowing for such comparison. For instance, Yeaman and Whitlock (2011)considered a fitness function similar to ours in a two-patch model, with a flexible parameter allowing to explore Laplace and Gauss trade-offs considered in our study. However, the effect of this parameter is not clearly discussed in their study.

Conclusion and perspective

We show that the process of genetic aggregation is a robust phenomenon when local adaptation evolves in a new environmental pocket. The detailed pattern of aggregation depends on both the emergence and the reconfiguration phase and vary depending on the precise shape of function relating trait values to fitness. The emergence of aggregation requires that several clines co-occur at the same spatial location. This situation may not systematically characterize ecological variation. For instance, it is possible that local adaptation occurs on ecological gradients (notably abiotic such as temperature, photoperiod etc.), rather than on "pockets" of habitats. In this case, staggered clines may evolve with little scope for genetic aggregation. However, the presence of an abiotic gradient does not necessarily translate into a gradient in optimal trait values in a given species. We have a limited knowledge of this variation. Moreover, many natural habitats may be better described as patches of different sizes rather than as gradients. In particular, anthropized landscapes may be characterized by the creation of marked segmentation and abrupt transition in habitat quality at moderate-to-coarse spatial grains (typically 0.1-1000 ha, Strayer 2005) due to infrastructures (e.g. roads), spatial heterogeneity in land use (e.g. crops in agricultural landscapes or stands within managed forests) and management practices (e.g. pesticide application). This first trend may combine with a homogeneization process at fine grain (typically <0.1 ha; Strayer 2005) in many contexts like urban areas (e.g. soil artificialization) or managed forest or agricultural ecosystems(e.g. Fraterrigo et al. 2005 and references therein). Hence, the combination of both processes suggests that the rapidly growing human imprint on landscape structure should often result in a marked patchiness, making spatially explicit models critical to consider when investigating patterns and dynamics of local adaptation in the field, and more generally adaptation and resilience of organisms to global changes.

Acknowledgements

We thank Noémie Harmand and Florence Débarre for discussions and comments.

References

Alleaume-Benharira, M., I. R. Pen, and O. Ronce. 2006. Geographical patterns of adaptation within a species' range: interactions between drift and gene flow. J. Evol. Biol. 19:203–215.

Anciaux, Y., L. M. Chevin, O. Ronce, and G. Martin. 2018. Evolutionary rescue over a fitness landscape. Genetics 209:265–279.

Barton, N. H., and G. M. Hewitt. 1989. Adaptation, speciation and hybrid zones. Nature 341:497–503.

Bridle, J. R., J. Polechova, M. Kawata, and R. K. Butlin. 2010. Why is adaptation prevented at ecological margins? New insights from individual-based simulations. Ecol. Lett. 13:485–

494.
Bürger, R., and A. Akerman. 2011. The effects of linkage and gene flow on local adaptation: A two-locus continent-island model. Theor. Popul. Biol. 80:272–288. Elsevier Inc.
Bürger, R., and M. Lynch. 1995. Evolution and Extinction in a Changing Environment: A Quantitative-Genetic Analysis. Evolution 49:151–163.
Charlesworth, B., and N. H. Barton. 2018. The spread of an inversion with migration and selection. Genetics 208:377–382.
Charlesworth, D. 2016. The status of supergenes in the 21st century: Recombination suppression in Batesian mimicry and sex chromosomes and other complex adaptations. Evol. Appl. 9:74–90.
Chevin, L. M., R. Lande, and G. M. Mace. 2010. Adaptation, Plasticity, and Extinction in a Changing Environment: Towards a Predictive Theory. PLoS Biol. 8:e1000357.
Débarre, F., and S. Gandon. 2010. Evolution of specialization in a spatially continuous environment. J. Evol. Biol. 23:1090–1099.
Flaxman, S. M., J. L. Feder, and P. Nosil. 2013. Genetic hitchhiking and the dynamic buildup of genomic divergence during speciation with gene flow. Evolution 67:2577–2591.
Fouqueau, L., and D. Roze. 2021. The evolution of sex along an environmental gradient. Evolution 75:1334–1347.
Fraterrigo, J. M., M. G. Turner, S. M. Pearson, and P. Dixon. 2005. Effects of past land use on spatial heterogeneity of soil nutrients in southern appalachian forests. Ecol. Monogr. 75:215–230.
Gomulkiewicz, R., and D. Houle. 2009. Demographic and genetic constraints on evolution. Am. Nat. 174.
Kirkpatrick, M., and N. Barton. 2006. Chromosome inversions, local adaptation and speciation. Genetics 173:419–34.
Kirkpatrick, M., and N. H. Barton. 1997. Evolution of a species' range. Am. Nat. 150:1–23.
Lande, R. 1976. Natural-Selection and Random Genetic Drift in Phenotypic Evolution. Evolution 30:314–334.
Lenormand, T. 2012. From local adaptation to speciation: specialization and reinforcement. Int. J. Ecol. 2012:e508458.
Lenormand, T. 2002. Gene flow and the limits to natural selection. Trends Ecol. Evol. 17:183–189.
Lenormand, T. 2003. The evolution of sex dimorphism in recombination. Genetics 163:811–822.
Lenormand, T., and S. P. P. Otto. 2000. The evolution of recombination in a heterogeneous environment. Genetics 156:423–438.
Marshall, D. J., S. C. Burgess, and T. Connallon. 2016. Global change, life-history complexity and the potential for evolutionary rescue. Evol. Appl. 9:1189–1201.
Martin, G., S. F. S. F. Elena, and T. Lenormand. 2007. Distributions of epistasis in microbes fit predictions from a fitness landscape model. Nat. Genet. 39:555–560. Nature Publishing Group, The Macmillan Building 4 Crinan Street London N 1 9 XW UK,.
Martin, G., and T. Lenormand. 2006a. A general multivariate extension of Fisher's geometrical model and the distribution of mutation fitness effects across species. Evolution 60:893–907.
Martin, G., and T. Lenormand. 2006b. The fitness effect of mutations across environments: a survey in the light of fitness landscape models. Evolution 60:2413–2427.
Martin, G., and T. Lenormand. 2015. The fitness effect of mutations across environments: Fisher's geometrical model with multiple optima. Evolution 69:1433–1447.
Matuszewski, S., J. Hermisson, and M. Kopp. 2015. Catch me if you can: Adaptation from standing genetic variation to a moving phenotypic optimum. Genetics 200:1255–1274.

Nagylaki, T. 1975. Conditions for the existence of clines. Genetics 80:595–615.

Nosil, P., D. J. Funk, and D. Ortiz-Barrientos. 2009. Divergent selection and heterogeneous genomic divergence. Mol. Ecol. 18:375–402.

Osmond, M. M., and C. A. Klausmeier. 2017. An evolutionary tipping point in a changing environment. Evolution 71:2930–2941.

Otto, S. P. 2009. The Evolutionary Enigma of Sex. Am. Nat. 174:S1–S14.

Otto, S. P. S. P., and T. Lenormand. 2002. Resolving the paradox of sex and recombination. Nat. Rev. Genet. 3:252–261. Nature Publishing Group.

Polechová, J., and N. H. Barton. 2015. Limits to adaptation along environmental gradients. Proc. Natl. Acad. Sci. U. S. A. 112:6401–6406.

Pylkov, K. V, L. A. Zhivotovsky, and M. W. Feldman. 1998. Migration versus mutation in the evolution of recombination under multilocus selection. Genet. Res. 71:247–256.

Ravigne, V., U. Dieckmann, and I. Olivieri. 2009. Live where you thrive: joint evolution of habitat choice and local adaptation facilitates specialization and promotes diversity. Am. Nat. 174:E141–E169.

Sardell, J. M., and M. Kirkpatrick. 2020. Sex differences in the recombination landscape. Am. Nat. 195:361–379.

Schwander, T., R. Libbrecht, and L. Keller. 2014. Supergenes and Complex Phenotypes. Curr. Biol. 24:R288–R294. Elsevier Ltd.

Slatkin, M. 1973. Gene flow and selection in a cline. Genetics 75:733–756.

Slatkin, M. 1978. Spatial patterns in the distributions of polygenic characters. J. Theor. Biol. 70:213–228.

Strasburg, J. L., N. A. Sherman, K. M. Wright, L. C. Moyle, J. H. Willis, and L. H. Rieseberg. 2012. What can patterns of differentiation across plant genomes tell us about adaptation and speciation? Philos. Trans. R. Soc. B Biol. Sci. 367:364–373.

Strayer, D. L. 2005. Challenges in Understanding the Functions of Ecological Heterogeneity BT - Ecosystem Function in Heterogeneous Landscapes. Pp. 411–425 *in* G. M. Lovett, M. G. Turner, C. G. Jones, and K. C. Weathers, eds. Springer New York, New York, NY.

Yeaman, S. 2013. Genomic rearrangements and the evolution of clusters of locally adaptive loci. Proc. Natl. Acad. Sci. U. S. A. 110:E1743–E1751.

Yeaman, S., S. Aeschbacher, and R. Bürger. 2016. The evolution of genomic islands by increased establishment probability of linked alleles. Mol. Ecol. 25:2542–2558.

Yeaman, S., and M. C. Whitlock. 2011. The genetic architecture of adaptation under migration-selection balance. Evolution 65:1897–1911.

Figures

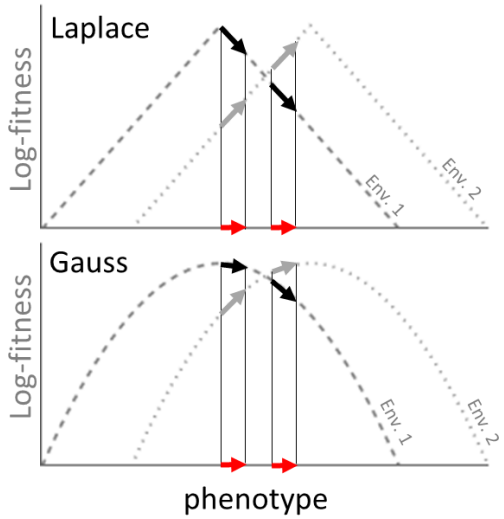

Fig. 1. Laplace and Gauss fitness functions. The red arrow represents a mutation increasing the trait value. With Laplace fitness function, the log-fitness gain of the mutation in environment 2 (gray arrow) is equal to the log-fitness loss in environment 1 (black arrow), irrespectively of the current phenotype (in absence of optimum overshoot). With Gauss fitness function, the log-fitness gains (and losses) depend on current phenotype.

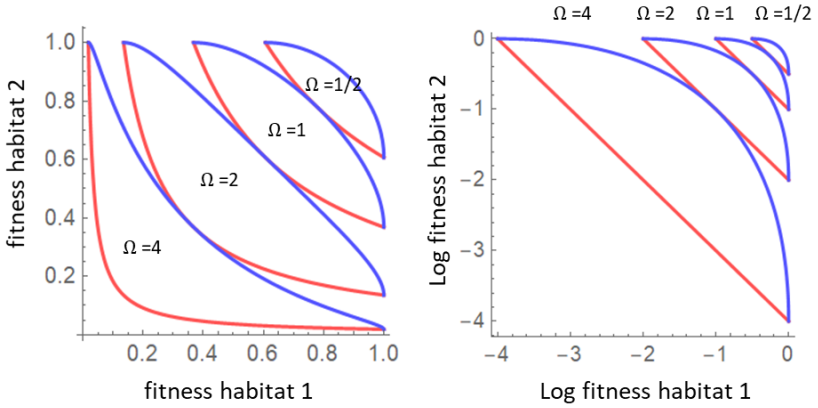

Fig. 2. Fitness trade-off curves between environments, for different intensity of stabilizing selection (Ω). Without loss of generality, delta z_{opt} = 1. Blue: Gaussian fitness function (γ = 2). Red: Laplace fitness function (γ = 1). Left : fitness; Right: log fitness.

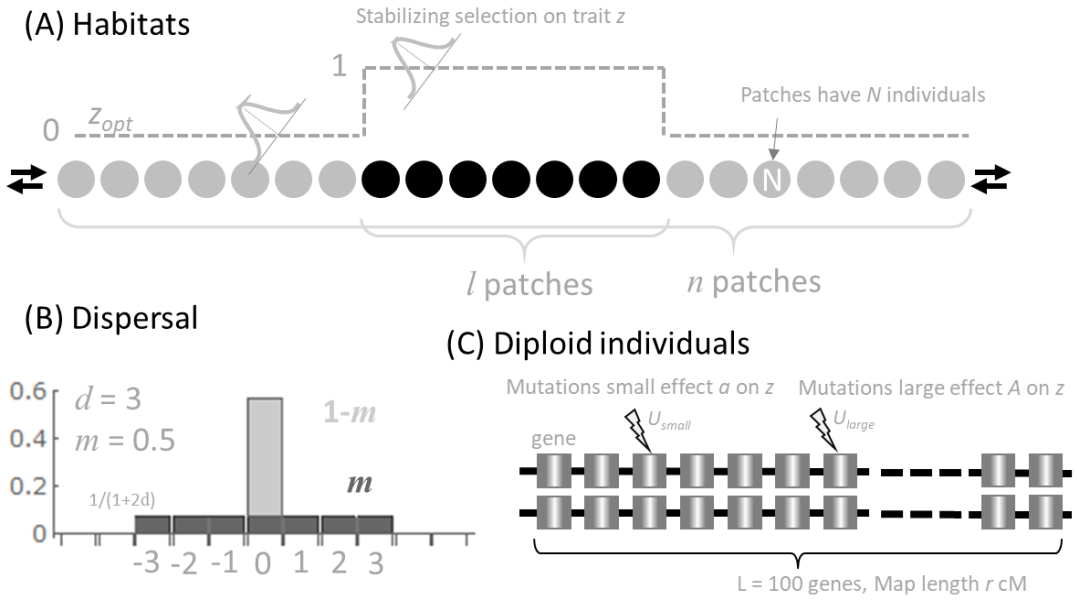

Fig 3. Model assumptions. (A) The landscape is one-dimensional and circular with n patches with N individuals. Habitat 1 and 2 are made of n-l and l contiguous patches with an optimal trait value $z_{opt} = 0$ and 1, respectively. Trait z is under stabilizing selection around this optimum. (B) Dispersion kernel. A proportion 1-m of individuals stay in their patch, and a proportion m is uniformly distributed among patches within distance d of the focal patch (focal patch included). Hence, each non-focal patch receives $m/(1+2d)$ migrants. (C) Individuals are diploid and have a pair of chromosomes with L loci determining trait z. Mutation of small or large effects can occur on all these loci.

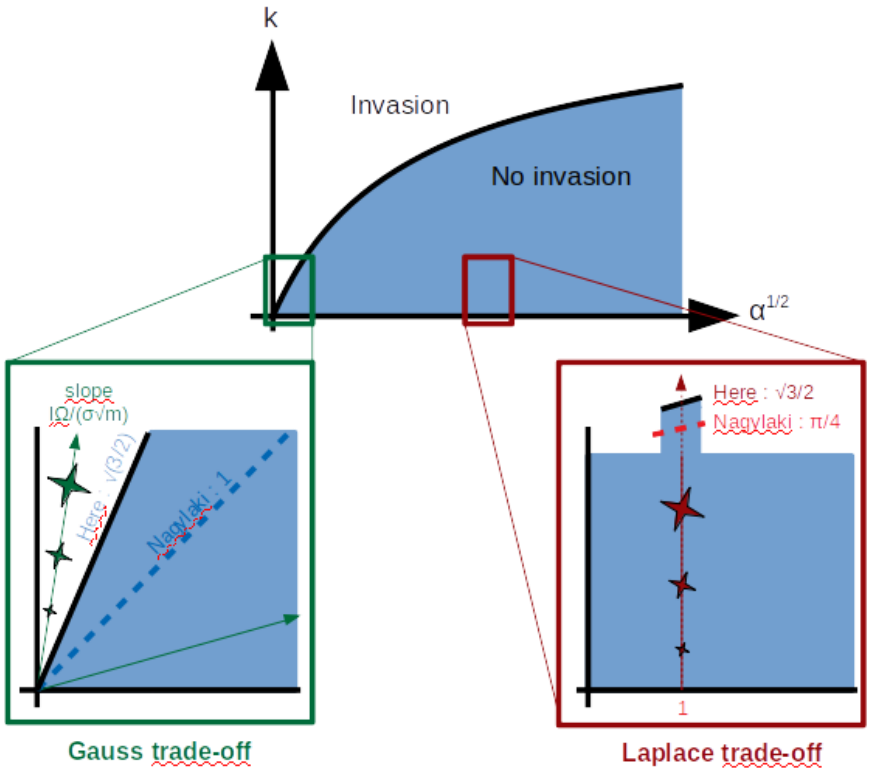

Fig 4. Conditions for polymorphism in the semi-infinite limit of our model. The upper panel correspond to the condition for the existence of a cline in an habitat 'pocket' as predicted using (Nagylaki 1975). See Lenormand (2002), Box 2, Fig II. The figure shows whether a mutant can invade (white area) or not (blue area) the $z^*=0$ resident phenotype as a function of two compound parameters k, and α (if it does, a cline establishes between the habitats). On the y-axis k measures the relative scales of the spatial heterogeneity (width of the pocket) and of the 'characteristic length' ($\sigma/\sqrt{s}$), which weighs the strength of selection relative to gene flow. On the x-axis, $\alpha^{1/2}$ measures the square root of the ratio of selection coefficients outside/inside the pocket. The lower panels zoom on areas of the figure where small mutants are positioned with a Gauss (green, left) and Laplace (red, right) fitness trade-off. In both panels, mutation with increasing phenotypic effects are presented using stars with increasing size. In the Gauss case, mutations of different effect sizes follow lines with zero intercept and slopes that depend on the parameters (see text). Mutants can invade if this slope is above the critical slope corresponding to the frontier between the blue and white areas. This is an all-or-nothing situation. Mutations of small and large effects can either all invade or none of them can invade. In the Laplace case, mutations are on a vertical line with $\alpha = 1$ (symmetry between habitats). Infinitesimal mutations cannot invade, but large mutations can form clines if their phenotypic effect is sufficiently large.

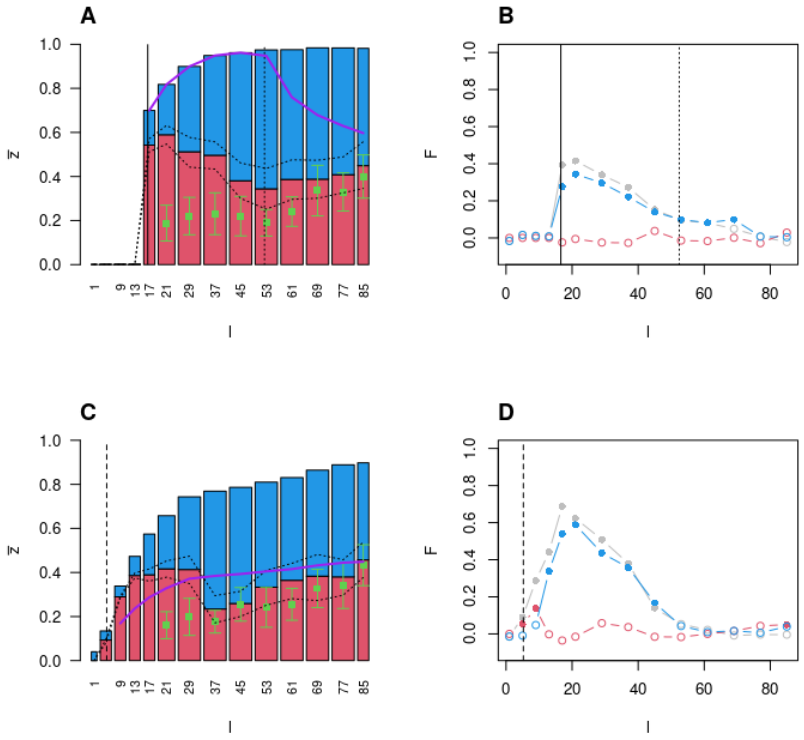

Fig 5. Short-term genetic architecture of local adaptation after the emergence phase. Composition and structure of adaptive genotypes at the center of habitat 2 after the initial phase of adaptation (see methods) for Laplace (panels A and B) and Gauss (panels C and D) fitness trade-off. Panels A and C present the average phenotype (bars) at the middle of habitat 2 for various sizes of habitat 2 (l), averaged over 20 replicates. The average relative contribution of alleles with large and small effects are presented in red and blue within each bar, respectively. Dotted black lines show a 95% confidence interval of these relative contributions. Green squares show the average contribution of large alleles in the corresponding control (removing habitat 1), along with a 95% confidence interval (1,96 × s.e. computed over 20 replicates). The purple line shows the expected contribution of large versus small effects computed when rare at emergence. In panel A and B (Laplace fitness function), vertical black lines show the analytical invasion thresholds above which a small (dotted line) or a large (solid line) effect mutation can invade alone the z^*=0 resident phenotype. In panel C and D (Gauss fitness function), the vertical black dashed line show the analytical invasion threshold above which a small or large mutation can invade alone the z^*=0 resident phenotype. Panels B and D present the average aggregation of adaptive alleles along the genetic map at the middle of habitat 2 for various sizes of habitat 2 (l), averaged over 20 replicates. Aggregation of all the adaptive alleles, small effects only and large effects only are presented in grey, blue and red, respectively. Filled dots correspond to significant F values, based on Bonferroni – corrected tests with 5% family-wise error rate.

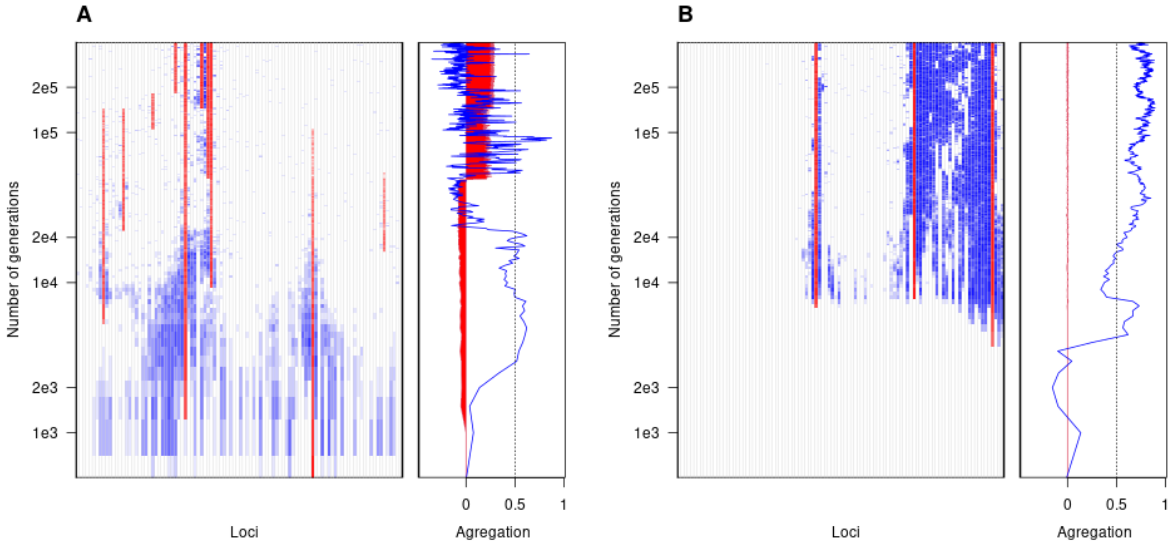

Fig 6. Typical examples of aggregation dynamics with Gauss (panel A) and Laplace (panel B) fitness functions. In each panel, the frequency of the dominant adaptive allele at each locus within the central deme of habitat 2 is presented, in blue if it is an allele with a small effect size, red if it is a large effect size, with darker color for larger frequency. The x-axis "loci" represent loci, as they are ordered on the chromosome The evolution of the genetic architecture through time can be observed along the y-axis (in log scale, which allows presenting simultaneously the emergence and long term reconfiguration phase). Right next to these maps, we present how the aggregation metrics of small (blue lines) and large effect size alleles (red shapes) change in time. In the two examples, the width of habitat 2 is set to l=19 demes (which is between the swamping limits for small and large effect mutations in the Laplace case, see Fig 5A).

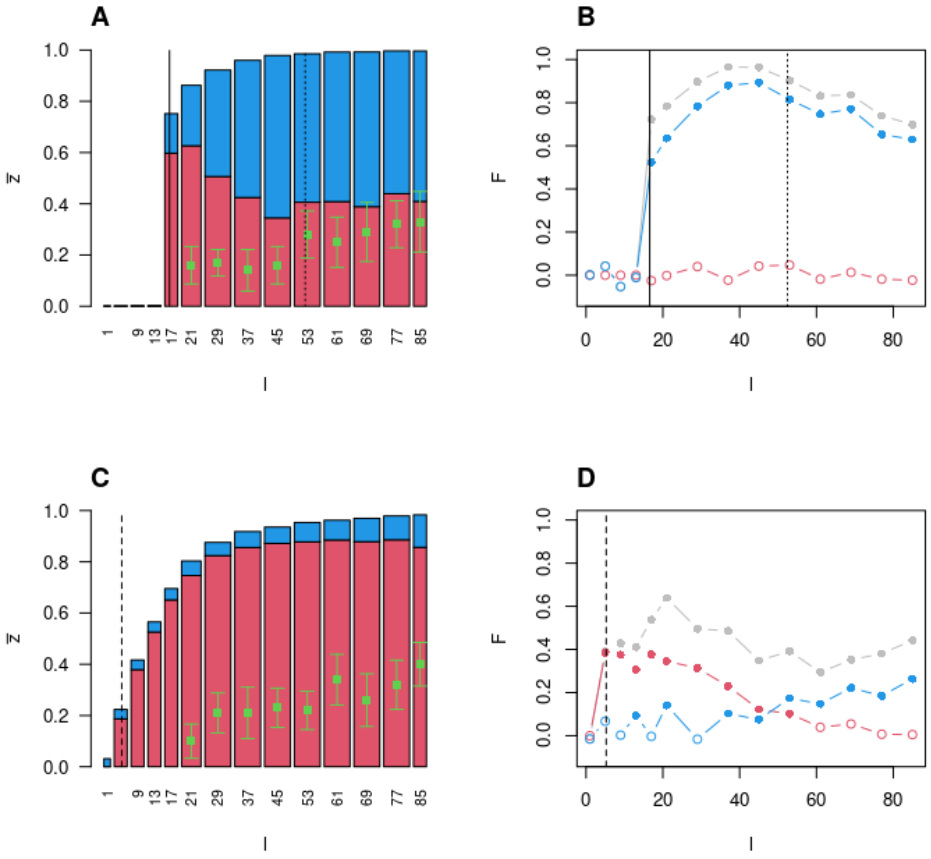

Fig 7. Long-term genetic architecture of local adaptation after the reconfiguration phase. The legend of the figure is identical than on Fig 5, except that measures are taken on the long term, after 400 000 generations.

Tables

Parameter	Definition	Values
X	Total number of patches	400
l	Number of patches of habitat 2	1,5,9,…,21, 29, 37,..., 85
N	Number of individuals within patches	100
m	Proportion of migrating juveniles	0.5
d	Maximum dispersal distance of migrants	10
γ	Shape of fitness around local optimum	1 (Laplace), 2 (Gauss)
Ω	Intensity of selection	1
L	Number of loci on the chromosome	100
a	Effect size of small mutations	0,.01
A	Effect size of large mutations	0.1
μ_a, μ_A	Mutation rates towards alleles of small and large effects	1e-5, 1e-8
T	Number of generations in a simulation	<50'000 (initial phase), 400'000 (long term)

Table 1. Parameter values used in simulations.

List of parameters values used in the simulations. We used fourteen values of l , for both long term and initial phase of adaptation, for both Laplace and Gauss fitness functions. We used 20 replicates per combination of parameter values. This resulted in $14 \times 2 \times 2 \times 20 = 1120$ simulations. For each simulation with $l \geq 21$, we performed a control simulation where habitat 1 was removed, which resulted in $9 \times 2 \times 2 \times 20 = 720$ control simulations. These control simulations were not performed for $l < 21$, because dispersal kernel with $d = 10$ (the value used throughout) was undefined in that case.